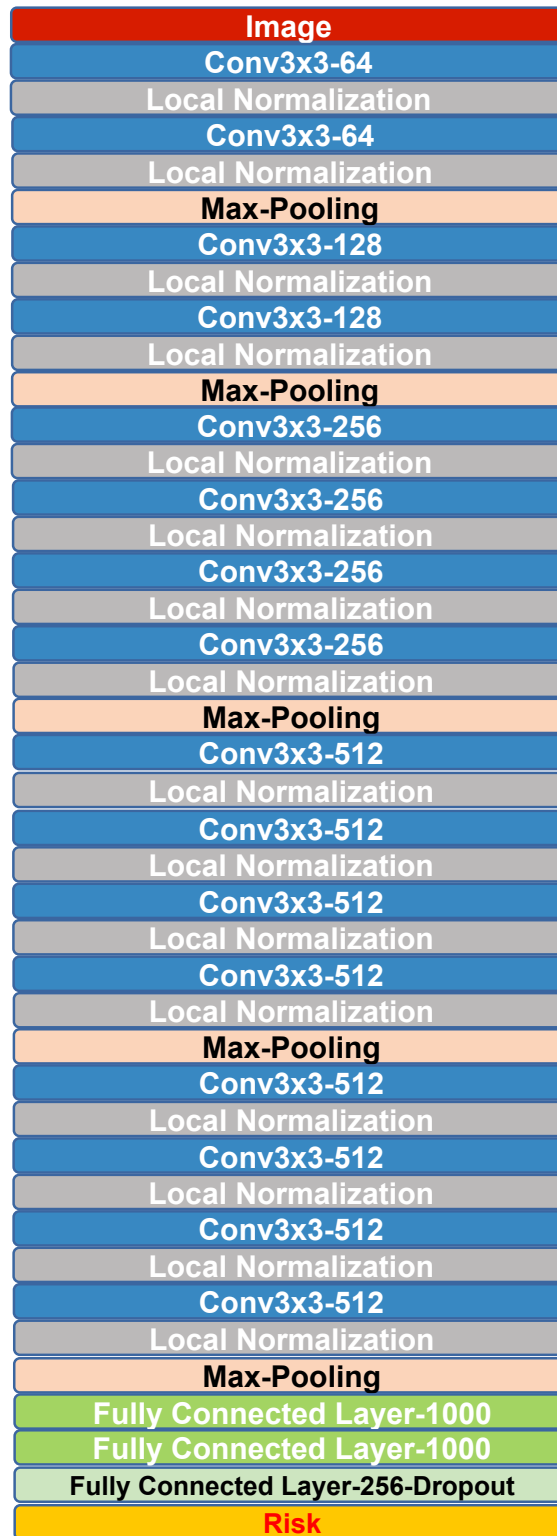


# Supporting Information

Mobadersany et al. 10.1073/pnas.1717139115



**Fig. S1.** Detailed diagram of the SCNN architecture. The architecture is a variation of the VGG network and combines convolutional, maximum pooling, local normalization, and fully connected layers.

Superficial integration of genomic variables with SCNN

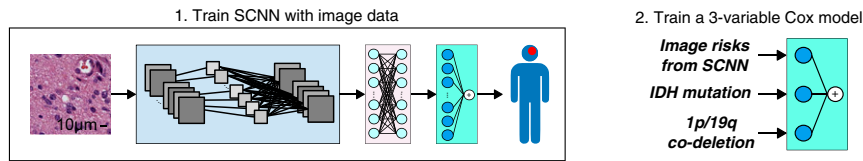


**Fig. S2.** Superficial integration of histology and genomic biomarkers. We evaluated the benefit of including genomic biomarkers in GSCNN training by evaluating the accuracy of a more superficial integration approach. We first trained an SCNN using histology images alone (step 1). After this training, we combined the risks produced by this SCNN with genomic variables using a simple linear Cox regression model. This Cox model was trained using the training samples and was evaluated on testing samples to measure prediction accuracy.

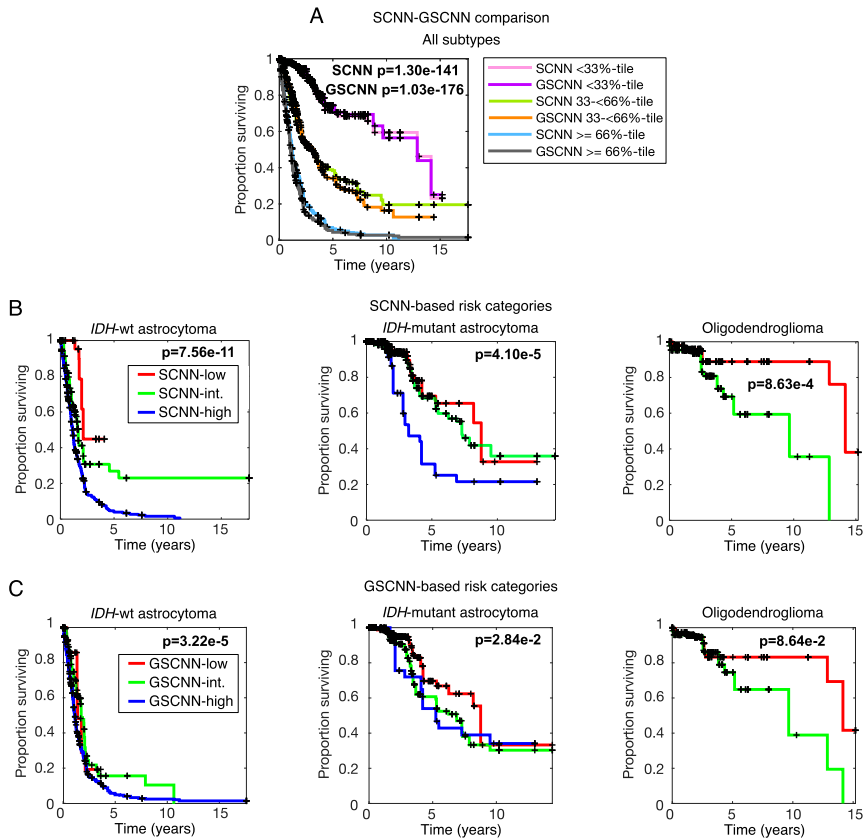


**Fig. S3.** Kaplan-Meier analysis of SCNN and GSCNN. (A) We compared the overall prediction power of SCNN and GSCNN in the samples from all subtypes using tertiles. Although the log rank test for GSCNN indicates slightly better separation of survival curves, visually, the curves for SCNN and GSCNN are remarkably similar. (B) SCNN risk categories perform well when examined within each molecular subtype. SCNN is not able to assign patients to these subtypes reliably, however, since its predictions are based entirely on histology. (C) GSCNN risk categories overlap significantly when examined in each molecular subtype. Although some separation is apparent, most of the predictive power of GSCNN comes from its ability to reliably assign patients to molecular subtypes.

**Table S1. Summary of dataset clinical features**

| Characteristic           | Total, <i>n</i> = 769 | Molecular subtype                           |   |  |
|--------------------------|-----------------------|---|---|--|
|                          |                       | Astrocytoma IDH WT,<br><i>n</i> = 335 (48%) | Astrocytoma IDH mutant,<br><i>n</i> = 220 (32%) | Oligodendroglioma,<br><i>n</i> = 142 (20%) |
| WHO histologic grade (%) |                       |   |   |  |
| II                       | 181 (25)              | 14 (4)                                      | 96 (48)   | 69 (53)                                    |
| III                      | 205 (28)              | 57 (17)                                     | 88 (44)   | 60 (46)                                    |
| IV                       | 350 (47)              | 262 (79)                                    | 17 (8)  | 1 (1)*                                     |
| Age at diagnosis, y      |                       |   |   |  |
| Range                    | 10–88                 | 10–88                                       | 14–73   | 17–75                                      |
| Median                   | 51 ± 15.5             | 58 ± 14.0                                   | 36 ± 11.3                                       | 45.5 ± 12.7                                |
| Sex, female (%)          | 308 (42)              | 137 (41)                                    | 86 (43)   | 54 (42)                                    |
| Median survival, y       |                       |   |   |  |
| Grade II                 | —                     | 2.1   | 8.2   | 14.2                                       |
| Grade III                | —                     | 1.7   | 6.3   | 9.7  |
| Grade IV                 | —                     | 1.2   | 3.0   | N/A  |

\*Grade IV is not defined for oligodendroglioma. This sample was initially classified as an astrocytoma under the older histological classification paradigm (before molecular subtyping). N/A, not applicable.

### Dataset S1. Patient summary and assignment to training and testing sets

[Dataset S1](#)